JOURNAL OF CATALYSIS **116**, 325–337 (1989)

The Role of Tellurium and Antimony in $PtTe/Al_2O_3$ and $PtSb/Al_2O_3$ Reforming Catalysts

CHI H. CHENG, KERRY M. DOOLEY, AND GEOFFREY L. PRICE[1]

Department of Chemical Engineering, Louisiana State University, Baton Rouge, Louisiana 70803

Received May 23, 1988; revised November 15, 1988

$PtTe/Al_2O_3$ and $PtSb/Al_2O_3$ bimetallic catalysts were studied using the model *n*-hexane isomerization, aromatization, and hydrocracking reactions at 673 K and the cyclohexane dehydrogenation reaction at 573 K, under atmospheric pressure in a recirculation batch reactor. An increase in the selectivity for isomerization (and a corresponding decrease in hydrocracking selectivity) was found for all coimpregnated $PtTe/Al_2O_3$ and $PtSb/Al_2O_3$ catalysts compared to Pt/Al_2O_3. The change in selectivity can be caused either by electronic effects, which increase the specific activities for isomerization, or by geometric effects, which reduce the rate of hydrocracking. The results of the kinetic experiments, along with FTIR spectroscopy of adsorbed CO using the isotopic dilution method, suggest that electronic effects can be identified with Te/Pt alloying in catalysts of low ($Te/Pt < 0.06$) Te content, while geometric effects predominate in catalyst formulations more concentrated in the post-transition metal. The dehydrogenation turnover frequencies were also enhanced at low Te/Pt ratio; in this respect the dehydrogenation and isomerization reactions are similar. Direct six-member ring closure, rather than ring expansion by way of an adsorbed methylcyclopentane intermediate, accounted for most of the production of benzene. $PtTe/Al_2O_3$ catalysts were also prepared by vapor deposition of Te onto Pt/Al_2O_3. These catalysts exhibited selectivities which were influenced by the type of carrier gas used to deposit the tellurium. A carrier gas containing *n*-hexane improved the selectivity relative to hydrogen or helium carrier gases. The mechanism of this selectivity effect is unknown but possibly due to carbon incorporation into a Pt–Te alloy.

INTRODUCTION

Bimetallic reforming catalysts have played an important role in petroleum refining processes over the last two decades. In most industrial applications the traditional reforming catalyst, Pt/Al_2O_3, has been modified by incorporating a second metal such as Re (*1*) or Ir (*2*). Some of the advantages offered by bimetallic catalysts include reduced rates of deactivation, higher reformate yields, and higher activities. Research on other bimetallic systems which may further improve the current reforming processes has not ended. Bimetallic systems such as PtAu (*3*) and PtCu (*4*) have been investigated and reported to provide desirable characteristics as reforming catalysts.

An important improvement which might be accomplished by alloying techniques is the suppression of hydrogenolysis or hydrocracking reactions thus resulting in an improvement in the C_5^+ liquid yields. Two theories (*5, 6*) are conceivable to explain the suppression of hydrogenolysis or hydrocracking reactions by alloying:

1. Geometric effect (dilution effect). Alloying of Pt with the other metal simply dilutes the Pt–Pt ensembles. The hydrogenolysis reaction, which requires multiple contiguous adsorption sites, is thereby suppressed.
2. Electronic effect (ligand effect). The electronic interaction between the Pt and the second metal alters the strength of the adsorbate bond to the adsorption site. The different chemisorption bond strengths result in altered catalytic activity and selectivity.

---

[1] To whom correspondence should be addressed.

0021-9517/89 $3.00

The post-transition metals of groups IVA, VA, and VIA have been considered candidate elements which can form bimetallic clusters with Pt to enhance desirable characteristics of reforming catalysts, e.g., selectivity to aromatics, activity, and activity maintenance. Catalysts containing Sb (*7*), Bi (*7*), S (*8*), Te (*9, 10*), Pb (*11*), Sn (*11, 12*), and Ge (*12*) have been examined recently by different investigators. Modification of Pt/Al_2O_3 by Sb or Bi (*7*) stabilizes the activity for cyclohexane dehydrogenation and *n*-heptane dehydrocyclization at high temperatures (723–773 K). Total catalytic activity and selectivity were shown to be a maximum when the Sb/Pt or Bi/Pt atomic ratio is 1/1. However, the catalysts are inactive at lower temperatures ($\approx$573 K). The authors suggested that the inhibition of hydrogenolysis reactions is due to the dilution of the Pt sites by the second metal component, while the lower temperature inactivity is caused by electronic effects. Similar results were found using $PtSn/Al_2O_3$ and $PtPb/Al_2O_3$ catalysts (*11*). These results are contrary to the earlier report on $PtSn/Al_2O_3$ by Davis *et al.* (*12*), who suggested that the change in selectivity is caused by changes in electronic density of the platinum atoms which weaken the Pt–C bond strength and thereby decrease rates of poisoning by coke.

Goldwasser and co-workers (*13*) studied the isomerization and hydrogenolysis reactions of *n*-butane catalyzed by $PtGe/Al_2O_3$ (1 wt% Pt and 0–1 wt% Ge). The specific hydrogenolysis activity decreases with increasing Ge content while that of isomerization is only weakly influenced. The results were attributed to electron donation from Pt to reduced Ge ions. In naphtha reforming at 773 K, Eberly (*9*) and Brignac and Swan (*10*) showed that, upon addition of 0.1 wt% of either Te or S to a 0.3 wt% Pt/0.3 wt% Re or Ir alloy, the yield to hydrocracking products decreased and the yield to aromatics increased. The product distributions and stabilities of these catalysts are strongly dependent on the reaction conditions and the metal alloy compositions, as well as on the catalyst preparation procedure.

In commercial reforming catalysts, chlorine is usually added in order to enhance the acidity of the support. These catalysts are termed bifunctional; that is, the metal and the support play important individual roles in the reaction network. However, Pt itself can catalyze hydroisomerization independently. To avoid complications in the present work, the Pt–Te and Pt–Sb alloys have been supported on nonchlorinated γ-Al_2O_3, which is shown to be relatively nonacidic. Both kinetic data and structural information concerning these catalyst formulations have been obtained.

EXPERIMENTAL

1. Catalyst Preparation

(a) Al_2O_3 used for all catalysts was Linde type 60-503. The manufacturer's reported composition is 99.85% Al_2O_3, 0.1% SiO_2, 0.003% Na_2O, 0.02% Fe_2O_3, and 0.005% SO_4 by weight. The surface area is 215 m^2/g and the pore volume is 0.71 cm^3/g as reported by the manufacturer.

(b) $PtTe/Al_2O_3$ catalysts were prepared using both vapor deposition and coimpregnation methods. In the vapor deposition technique, highly dispersed Cl^--free Pt/Al_2O_3, prepared by ion exchange of $[Pt(NH_3)_4](OH)_2$ with Al_2O_3 (*14, 15*), was placed in a Pyrex-glass vessel of a recirculation batch reactor system and reduced with H_2 at 673 K. Elemental tellurium, which was placed upstream of the Pt/Al_2O_3 bed and heated to vaporize the Te, was carried by H_2, He, or a model compound reforming feed stream (a mixture of *n*-hexane, H_2, and He), and deposited onto the Pt/Al_2O_3 at 673 K. A high flow rate ($\approx$25 cc/s) of carrier gas caused most of the Te to bypass the bed, while at a low flow rate the entrance to the bed was more heavily tellurided than was the exit. A uniformly tellurided catalyst was preferred; therefore, high flow rates were used. Analysis by atomic absorption determined that the Pt content was 0.7–0.8 wt%, and the Te/Pt atomic ratios were found to be 0.14–0.40. These measurements indicated that one-third to one-half of the original Te was successfully deposited.

Coimpregnated, nonchlorinated PtTe/Al_2O_3 was prepared by coimpregnation of an acid solution of $H_2PtCl_6 \cdot 6H_2O$ and $H_2TeO_4 \cdot 2H_2O$ on the porous support. The catalyst was dried overnight in an oven maintained at 393 K and was reduced using flowing H_2 at 673 K for 15 hr. In order to remove chlorine, the solids were washed thoroughly with 5% ammonia (*16*) and deionized water. Final overnight drying was at 393 K. The catalyst contained 1 wt% Pt and the Te/Pt atomic ratio was varied from 0.0 to 1.2.

(c) PtSb/Al_2O_3 was prepared by the coimpregnation method as described above, with the exception that the solution contained $H_2PtCl_6 \cdot 6H_2O$ and $SbCl_3$. The Sb/Pt atomic ratio was varied from 0.0 to 1.24 and the Pt content was 1.1 wt%.

The chlorine content of three typical (co)impregnated catalysts, Pt/Al_2O_3, PtTe/Al_2O_3 (Te/Pt = 0.06), and PtSb/Al_2O_3 (Sb/Pt = 0.67), was found to be 80, 50, and 130 ppm, respectively, using X-ray fluorescence kindly provided by Exxon Research and Development in Baton Rouge, Louisiana. These measurements indicate that relatively small amounts of chlorine were present as anticipated.

A thermogravimetric analyzer (Perkin–Elmer TGA 7) was used to determine the reducibility of telluric acid. H_2TeO_4 was reduced to the zero valent state in flowing hydrogen at 673 K after a time period of about 12 hr, though this time period was impossible to measure accurately because elemental Te also vaporizes slowly and is observed as a mirror on the cool sections of the quartz enclosure. The low metal content of the supported catalyst prevented us from obtaining similar results on the actual catalyst. However, reduction of the actual catalyst should require less time as the surface area of H_2TeO_4 is greatly enhanced upon dispersion on the Al_2O_3 support.

2. *Blank Runs*

The catalytic activity of 200 mg of ammonia-washed Al_2O_3 was examined at 673 K using 3.3 kPa hydrocarbon (*n*-hexane, methylcyclopentane, cyclohexane, or 1-hexene), 59 kPa H_2, and He to atmospheric pressure. No product formation was observed for the *n*-hexane, methylcyclopentane, or cyclohexane reactions after 2 hr on stream. Carbon skeletal isomerization of 1-hexene was less than 5% after 2 hr on stream, although 1-hexene was readily converted to double-bond isomers (2- and 3-hexene). Similar results were obtained using Sb/Al_2O_3 catalysts. Tellurium is not stable on Al_2O_3 at 673 K; therefore, Te/Al_2O_3 could not be tested. These results suggest that the global activities for all the catalysts studied in this work can be attributed to the Pt metal function.

3. *Chemisorption of H_2 and CO*

Chemisorption capacities of all catalysts were determined with H_2 and CO. The published ratios H/Pt = 1, CO/Pt = 1.15 for Pt/Al_2O_3, and CO/Pt = 1.0 for PtTe/Al_2O_3 and PtSb/Al_2O_3 were employed to calculate the metallic dispersion (*17–19*). The adsorption isotherms were obtained at 298 K and pressures ranging from 10 to 10^4 Pa. Langmuir-type isotherms were obtained when H_2 was used as the adsorbate. However, when CO was used, a double adsorption isotherm method was required in order to take into account the weakly bound fraction (*20*).

Before each experiment, the catalyst was first treated with flowing H_2 for at least 3 hr at 673 K, followed by evacuation at 673 K ($<10^{-6}$ Torr) for 2 hr, then cooling. The isotherm was determined using an all-glass, static volumetric apparatus with pressures given by a 10- to 10^4-Pa diaphragm gauge (MKS).

It should be mentioned that the chemisorption experiments on the vapor deposited PtTe/Al_2O_3 catalysts were performed

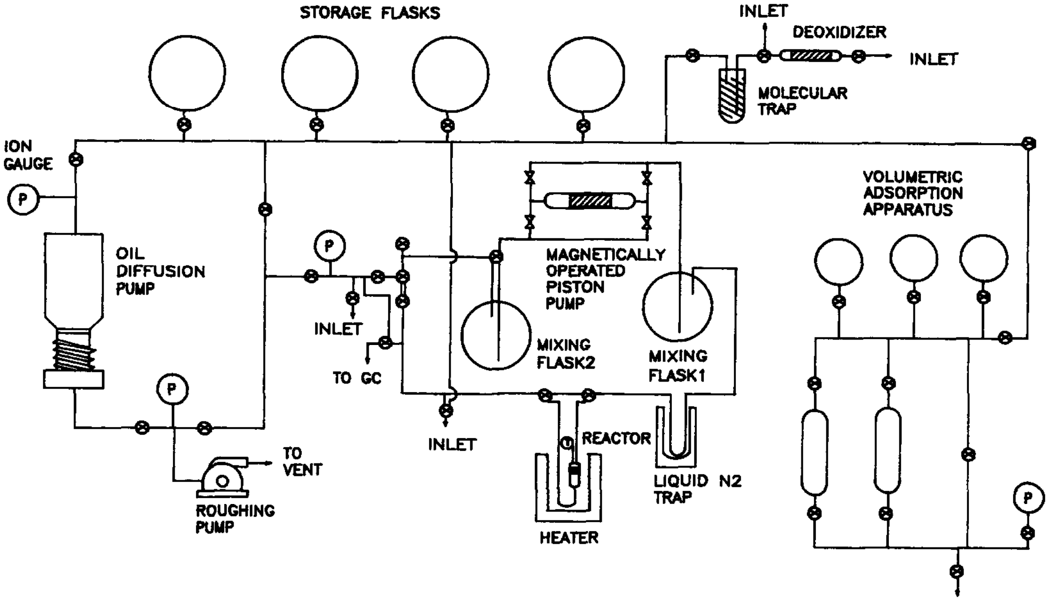

FIG. 1. Recirculation batch reactor system.

after test reactions. Therefore, effect of carbonaceous deposits on the adsorption capacity of the Pt active sites cannot be excluded.

4. Catalytic Reactions

A recirculation batch reactor with gas chromatographic (GC) analytical facilities (Carle Model 111H) was used. Total system volume was 580 cc and the calculated displacement rate of the pump was approximately 25 cc/s. A schematic diagram of the system is shown in Fig. 1. Partial pressures of reactants and products could be followed with respect to time by this arrangement. Reaction products could also be identified by GC–MS as necessary. The observed reaction rates of catalysts of two different particle sizes were similar at the reaction conditions, and calculations based on the methods of Wheeler (*21*) indicated that mass transfer limitations on catalyst operation were insignificant. A standard mixture of reaction components for GC calibration, used in conjunction with a mass balance for each sample taken, ensured that the accuracy of the data are within ±5%.

Before each reaction experiment, 20 to 200 mg of the catalyst was reduced with H_2 at 673 K for at least 13 hr with a liquid N_2 trap placed in the recirculation loop to remove water. The temperature of the catalyst was controlled by a PID controller (Love Model 151), with a reproducibility of ±1 K. Following activation, the rest of the system was evacuated, and then the system was filled with 3.3 kPa *n*-hexane or cyclohexane, 59 kPa H_2, and He to 107 kPa. The reaction mixture was sampled periodically and analyzed by GC. Cyclic hydrocarbons were separated by a 6-m 15% Carbowax on Chromosorb column. A 2-m Chromosorb 102 column and a 5-m 23% SP-1700 column were used to separate light gases (H_2, C1, and C2) and C3–C6 alkanes, respectively. All columns were maintained at 364 K. For the *n*-hexane reaction, the results using different catalysts were interpreted based on 30% conversion of *n*-hexane unless otherwise specified. The products were grouped as aromatic (benzene), isoparaffins [2- and 3-methylpentane (MP)], methylcyclopentane (MCP), and cracking products (the C1–C5 paraffins). Pt/Al_2O_3 catalysts, prepared by ion-exchange and impregnation methods, were used for the comparisons with vapor-deposited PtTe/Al_2O_3 and coimpregnated catalysts, respectively. The initial activities for the isomerization and cracking reactions of the catalysts were determined by the initial slopes of the product vs time accumulation curves. It was assumed that the active sites available for the reactions are those which can adsorb H_2 or CO; therefore, the catalytic activities are reported as mole hydrocarbon converted per time per mole surface Pt atom. This calculation, based on the initial slopes of the accumulation curves, is no better than ±15%, but it provides data for rudimentary comparisons of rate and selectivity.

5. *Characterization by FTIR*

The isotopic dilution method (*22–24*) was employed to determine the relative contributions of geometric and electronic effects resulting from alloying with Te or Sb promoters. The method can be explained briefly as follows. Assuming only a single Pt atom on the support, a CO molecule adsorbed on this atom exhibits a characteristic isolated C–O stretching band frequency. However, on the real catalytic surface, each Pt atom is surrounded by other Pt atoms and by additional X atoms for PtX/Al_2O_3 catalysts. Two effects on this band frequency result, namely dipole–dipole coupling and an electronic effect related to PtX alloying. The dipole–dipole coupling is an interaction force between adsorbed CO molecules which is inversely proportional to intermolecular distance cubed (*25*) and which results in a higher band frequency than the isolated band frequency. In the presence of electronic effects related to Pt–X alloying, changes from the isolated stretching band frequency depend on electron transfer between the outer orbitals of X and the Pt *d*-orbitals. If there is electron donation from X to Pt orbitals, then back donation from Pt to the CO antibonding orbitals causes the weakening of the CO bond and therefore decreases the band frequency. On the other hand, if X withdraws electrons from Pt, the band frequency will shift to a higher value. Dipole–dipole coupling can be eliminated by adsorbing a dilute gas mixture of ^{12}CO in ^{13}CO on the surface, since the coupling between Pt–^{12}CO and Pt–^{13}CO is negligible. Any observed differences in band frequencies for CO adsorbed on Pt/Al_2O_3 and PtX/Al_2O_3 at this condition of isotopic dilution can therefore be ascribed to the electronic effects of alloying. Experimentally, it is impossible to observe band frequencies at infinite dilution because the absorbance of the ^{12}CO band is too small. Alternatively, it is customary to extrapolate the curves for CO band frequency vs gas mixture composition to infinite dilution.

The IR experiments were conducted *in situ*, employing a UHV cell in which the catalyst can be heated, evacuated, and exposed to the gas phase. A schematic diagram of this cell is shown in Fig. 2. The wafer, 13 mm in diameter, was prepared by pelletizing 20 mg of the catalyst at 100 MPa. It was pretreated with flowing H_2 at 673 K for at least 13 hr, evacuated at the same temperature for 3 hr, and cooled to room temperature under dynamic vacuum. Then 2.7 kPa of the gas mixture of ^{12}CO and ^{13}CO was admitted to the cell, which after 15 min was evacuated to about 10 Pa. The IR spectra were recorded on an IBM IR/32 FTIR instrument. These procedures were determined based on the reproducibility of the data.

RESULTS

1. *Chemisorption of H_2 and CO*

The accessible Pt metal fractions of all the catalysts were determined by chemisorption of H_2 and CO. The support, Al_2O_3, Te/Al_2O_3, and Sb/Al_2O_3 showed no or insignificant adsorption capacity at the same conditions. The results of H_2 and CO chemisorption were similar for the coimpregnated PtTe/Al_2O_3 and PtSb/Al_2O_3; these results are given in Fig. 3. The

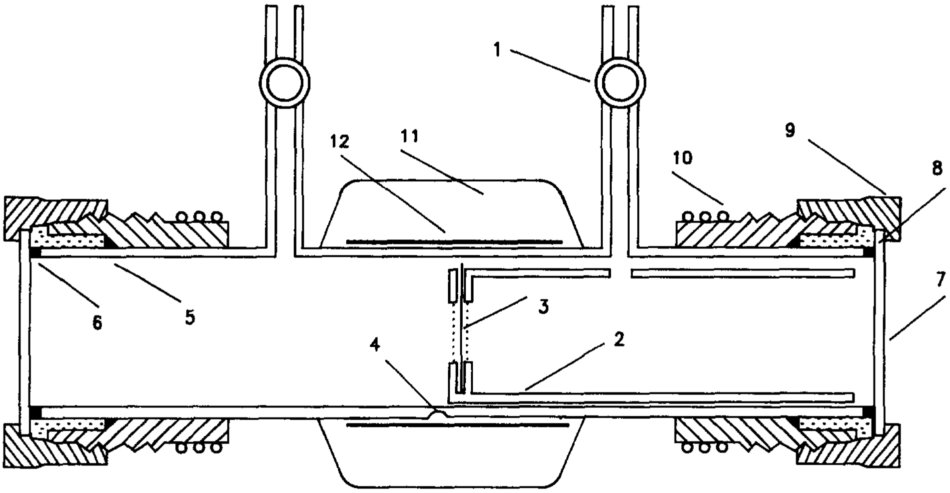

FIG. 2. High vacuum IR cell. Capability: $P = 10^{-4}$ Pa, $T = 820$ K. 1, High vacuum stopcock; 2, sample holders; 3, catalyst wafer; 4, thermocouple, 5, 6, viton o-rings; 7, NaCl window; 8, window attached to sleeve; 9, cajon ultra-Torr adaptor; 10, cooling water tubing; 11, thermal insulation; 12, heating wire.

amounts adsorbed decrease with increasing post-transition metal content; a dramatic fall in adsorption capacity is evident upon initial addition of Te or Sb. Te inhibits the adsorption more strongly than does Sb.

When the same experiments were performed on $PtTe/Al_2O_3$ catalysts prepared by vapor deposition, insignificant amounts of H_2 were adsorbed. The CO uptake, however, was approximately 20 to 30% of that on Pt/Al_2O_3. The PtTe bimetallic clusters formed using coimpregnation and vapor deposition methods are therefore different. This is further demonstrated by the catalytic results, reported below.

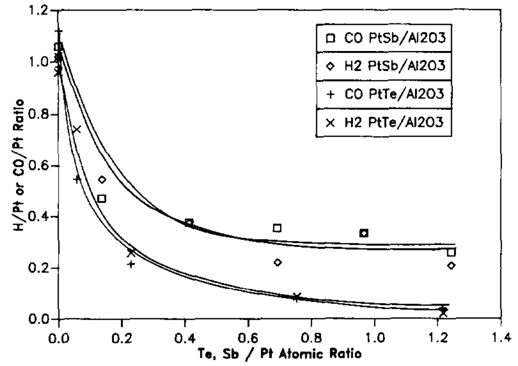

FIG. 3. Chemisorption of H_2 and CO on $PtTe/Al_2O_3$ and $PtSb/Al_2O_3$, measured at 298 K. Coimpregnated catalysts.

2. *n-Hexane Reaction*

(*a*) *Vapor-deposited* $PtTe/Al_2O_3$. The deposited Te is not completely stable for the duration of the activation periods and reaction experiments. A film of Te was visually observed on the downstream cold wall of the glass reactor. The Te content which is reported was determined by atomic absorption spectroscopy after the test reactions. The initial Te content was roughly two to three times the final, stable values.

In order to determine the dependence of the catalytic behavior on Te content and method of deposition (using different carrier gases), each catalyst was subjected to several test reactions at the same conditions, 673 K and 3.3 kPa initial pressure of *n*-hexane. Between each test reaction, the catalyst was treated with 57.8 kPa H_2 and He to 107 kPa for at least 12 hr. In Tables 1 and 2, the yield to hydrocracking and isomerization products for the different catalysts are compared based on 30% conversion of the reactant *n*-hexane. Typical

TABLE 1

Yield Percentage to Cracking Products, $PtTe/Al_2O_3$ (Vapor Deposition) Catalysts[a] at 673 K

Carrier gas	Te/Pt	Time[b]	Yield percentage at 30% conversion				
			1st[c]	2nd	3rd	4th	5th
He	0.37	77	6.6	3.8	3.4	3.4	3.5
He	0.24	110	6.3	5.0	4.3	4.5	—
H_2	0.38	38	8.1	4.2	4.7	5.2	—
Re[d]	0.40	325	3.0	3.1	3.4	—	—
Re[d]	0.14	350	3.0	3.4	4.5	5.2	5.6
H_2 + He	0.00	20	8.9	—	—	—	—

[a] Catalysts, 0.1 g, 0.7 wt% Pt.

[b] Time to reach 30% conversion for the first test reaction (min).

[c] Test number.

[d] A "reforming" gas mixture consisting of 3.3 kPa *n*-hexane, 57.8 kPa H_2, and He to 107 kPa.

product distributions obtained using Pt/Al_2O_3 and $PtTe/Al_2O_3$ are given in Table 3. The yields reported in the tables are mole percent of reactant converted to products. As indicated in Table 3, the addition of Te to Pt/Al_2O_3 generally increased the yield to isomerization products (2-MP and 3-MP) at the expense of both dehydrocylization and hydrocracking products. The overall activity also decreased by about one order of magnitude. These changes in product distribution took place only after the PtTe catalysts were exposed to a feed stream which included *n*-hexane at 673 K. The $PtTe/Al_2O_3$ catalysts which were prepared using a H_2 or He carrier gas initially exhibited higher yields to hydrocracking products (Table 1); these yields decreased in successive runs (in which *n*-hexane was the primary reactant). The selectivity toward isomerization products eventually approached a steady value which was considerably higher than that of Pt/Al_2O_3 (Table 2). However, when a feed stream containing *n*-hexane was used as the carrier gas for Te deposition, the $PtTe/Al_2O_3$ immediately displayed a high selectivity for isomerization products. The yield to hydrocracking products for these catalysts was the lowest among all those tested; but for those samples of low Te/Pt ratio (0.14), the yield to hydrocracking products increased in successive reactions. This activation phenomenon was not observed for the other catalysts of higher Te content, whose selectivities remained relatively constant. Finally, it is noted that the fragmentation pattern for hydrogenolysis products is also altered upon Te addition. $PtTe/Al_2O_3$ displays a clear preference for scission of in-

TABLE 2

Yield Percentage to 2MP + 3MP, $PtTe/Al_2O_3$ (Vapor Deposition) Catalysts[a] at 673 K

Carrier gas	Te/Pt	Time[b]	Yield percentage at 30% conversion				
			1st[c]	2nd	3rd	4th	5th
He	0.37	77	14.2	17.8	19.8	19.7	19.6
He	0.24	110	17.6	16.9	19.1	19.7	—
H_2	0.38	38	11.1	15.8	14.7	15.2	—
Re[d]	0.40	325	18.5	18.1	18.1	—	—
Re[d]	0.14	350	21.9	19.1	18.7	15.6	15.3
H_2 + He	0.00	20	12.0	—	—	—	—

[a] Catalysts, 0.1 g, 0.7 wt% Pt.

[b] Time to reach 30% conversion for the first test reaction (min).

[c] Test number.

[d] A reforming gas mixture consisting of 3.3 kPa *n*-hexane, 57.8 kPa H_2, and He to 107 kPa.

TABLE 3

Product Yields, Pt/Al_2O_3 and $PtTe/Al_2O_3$ Catalysts at 673 K

	Pt/Al_2O_3	$PtTe/Al_2O_3$[a]	
Time (min)	20	325	95
C1	0.69	≈0.00	≈0.00
C2	1.01	0.59	0.34
C3	2.50	0.95	0.45
i-C4	0.14	0.49	≈0.00
n-C4	1.78	0.61	0.33
i-C5	0.38	≈0.00	≈0.00
n-C5	2.40	0.36	≈0.00
ΣC1–C5	8.9	3.0	1.12
i-C6	12.0	18.5	6.88
MCP	6.0	6.6	3.18
Benzene	3.1	1.9	0.52
% Conversion	30.0	30.0	11.7

[a] The carrier gas was a reforming mixture consisting of 3.3 kPa *n*-hexane, 58.7 kPa H_2, and He to 107 kPa. Final Te/Pt atomic ratio was 0.40.

TABLE 4

Product Yields, $PtTe/Al_2O_3$ (Coimpregnation) Catalysts at 673 K

Catalyst[a] Te/Pt	Wt cat. (mg)	Rxn time (min)	Yield percentage at 30% conversion			
			2MP + 3MP	C1–C5	MCP	Benzene
0.00	20	43	7.2	11.0	6.0	5.8
0.06	20	40	11.6	6.3	6.6	5.5
0.23	100	39	11.2	6.8	6.8	5.2
0.76	200	51	12.5	7.1	6.4	4.0
1.2	200	80	11.3	8.4	6.3	4.0

[a] Pt 1 wt%.

TABLE 5

Initial Rates of Isomerization, Cracking (*n*-Hexane, 673 K), and Dehydrogenation (Cyclohexane, 573 K)

Catalyst	Initial rate (mol of reactant/s/surf.Pt) × 10^2		
	Isomerization	Cracking	Dehydrogenation
Pt/Al_2O_3	3.4	4.8	58
$PtTe/Al_2O_3$			
Te/Pt			
0.06	7.7	5.3	99
0.23	3.8	2.1	62
0.76	3.6	1.6	68
$PtSb/Al_2O_3$			
Sb/Pt			
0.14	3.4	1.0	41
0.41	4.0	1.5	39
0.69	3.3	0.8	32
0.97	2.6	0.9	40
1.24	3.0	1.5	43

ternal C–C bonds instead of terminal cleavage; such hydrocracking leads primarily to the formation of C2–C4 products.

(*b*) *Coimpregnated* $PtTe/Al_2O_3$. $PtTe/Al_2O_3$ prepared by the coimpregnation method exhibited even greater stabilities than vapor-deposited $PtTe/Al_2O_3$ during reaction experiments. No tellurium was evolved from the catalyst surface during these tests. The product distribution results for these catalysts at 673 K and 30% conversion of *n*-hexane are given in Table 4. Similar to the $PtTe/Al_2O_3$ catalysts prepared by vapor deposition, the use of coimpregnated catalysts caused a decrease in the yield to cracking products, thereby favoring the formation of isomerization products. The product compositions of methylcyclopentane and benzene were similar for all the catalysts. Note that even the introduction of a small amount of Te (Te/Pt atomic ratio = 0.06) was sufficient to dramatically alter the selectivities for isomerization and hydrocracking.

The initial rates of these coimpregnated catalysts for isomerization and hydrogenolysis are given in Table 5. At low Te content, the turnover frequency of Pt/Te catalysts for isomerization is significantly higher than that of Pt/Al_2O_3, while the cracking activity of both catalysts is practically the same. Therefore, the increase in the isomerization selectivity is due to an increase in isomerization activity. However, at high Te content, the increase in isomerization selectivity observed for PtTe catalysts is due more to a decrease in hydrocracking activity.

(*c*) *Coimpregnated* $PtSb/Al_2O_3$. The product distributions for *n*-hexane conversion using coimpregnated $PtSb/Al_2O_3$ catalysts are given in Table 6, and the initial turnover frequencies for isomerization and hydrocracking are provided in Table 5. Similar in behavior to the coimpregnated $PtTe/Al_2O_3$ catalysts, the Sb-containing bimetallics display a substantial increase in the yield to isomerization products by inhibiting the hydrogenolysis reactions, when compared to Pt/Al_2O_3 (Table 6). The yield to cyclic products is relatively constant with respect to Sb/Pt ratio. As shown in Table 5, the changes in observed selectivi-

TABLE 6

Product Yields, $PtSb/Al_2O_3$ (Coimpregnation) Catalysts at 673 K

Catalyst[a] Sb/Pt	Wt cat. (mg)	Rxn time (min)	Yield percentage at 30% conversion			
			2MP + 3MP	C1–C5	MCP	Benzene
0.0	20	43	7.2	11.0	6.0	5.8
0.14	50	44	12.8	5.1	6.8	5.3
0.41	50	70	13.5	5.4	6.7	4.4
0.69	50	108	15.4	4.5	6.6	3.5
0.97	50	115	13.7	5.1	6.8	4.4
1.24	50	120	13.9	4.5	7.4	4.2

[a] Pt 1.1 wt%.

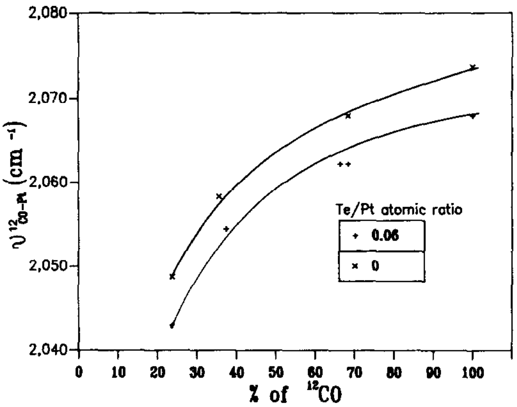

FIG. 4. Isotopic dilution experiments, coimpregnated catalysts.

ties using the PtSb/Al_2O_3 catalysts can be attributed to a decrease in the rate of hydrocracking.

3. Cyclohexane Reaction

The dehydrogenation activity for cyclohexane catalyzed by coimpregnated PtTe/Al_2O_3 and PtSb/Al_2O_3 has been investigated at 573 K. The results are presented in Table 5. Benzene was found to be the only dehydrogenation product for all the catalysts. No or insignificant amounts of hydrogenolysis products were observed, even at high conversion (>90%). The low-Te-content PtTe/Al_2O_3 has a higher dehydrogenation activity than Pt/Al_2O_3. High-Te-content catalysts exhibit dehydrogenation activity at about the same levels as Pt/Al_2O_3, while PtSb/Al_2O_3 shows moderately lower dehydrogenation activities.

4. FTIR

(*a*) *Coimpregnated PtTe/Al_2O_3*. The isotopic dilution method was employed to examine the relative importance of geometric and electronic effects in the behavior of coimpregnated PtTe/Al_2O_3 catalysts. These results suggest the absence of phase separation because only a single Pt–^{12}CO peak appeared (≈2040–2080 cm^{-1}) at the adsorption temperature. Only the set of data for the low Te/Pt atomic ratio (0.06) catalyst is presented in Fig. 4; the higher Te/Pt atomic ratio catalysts exhibited a peak of such low intensity that the data were not reliable. On the basis of these data, an electronic effect is possibly in operation because the band frequency curves for Pt/Al_2O_3 and PtTe/Al_2O_3 apparently do not coincide at infinite dilution, though scatter in the data makes the extrapolation somewhat uncertain (Fig. 4). Geometric effects are seemingly minimal for this low-Te-content catalyst, because the two curves are separated by almost equal frequencies at every percentage of ^{12}CO. The PtTe/Al_2O_3 curve lies below Pt/Al_2O_3, suggesting that electrons have been transferred from tellurium *s*- or *p*-orbitals to platinum *d*-orbitals. This electron transfer increases the back-donation of electrons to the CO antibonding orbitals and thereby decreases the CO bond strength. Such a phenomenon has been observed for PtSn/Al_2O_3 and PtPb/Al_2O_3 (*22*, *26*), but is contrary to that observed for PtS/Al_2O_3 (*27*) (electron withdrawal by S from Pt) and PtCu/Al_2O_3 (*23*) (no observable electronic effects).

(*b*) *Coimpregnated PtSb/Al_2O_3*. The isotopic dilution method for PtSb/Al_2O_3 gave results which differed from those of PtTe/Al_2O_3 (Fig. 5). All of the band frequencies for CO adsorbed on PtSb/Al_2O_3 converge to the frequency associated with adsorption

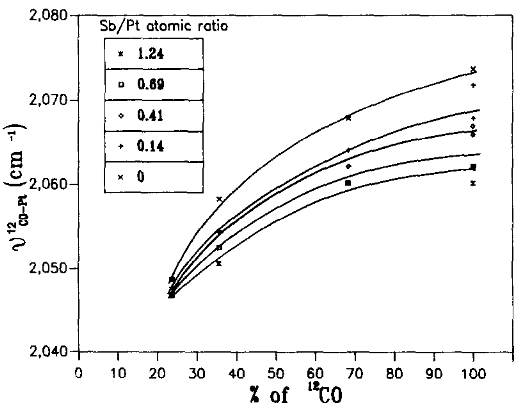

FIG. 5. Isotopic dilution experiments, coimpregnated catalysts.

on Pt/Al_2O_3 at infinite dilution. Therefore all band frequency deviations at higher ^{12}CO amounts are attributable to dipole–dipole coupling. This behavior is similar to that found using $PtCu/Al_2O_3$ (*23*).

DISCUSSION

The inhibition of gas uptake (Fig. 3) is possibly caused by partial poisoning of Pt active sites by Te or Sb. Catalyst poisoning can be considered a "geometric" effect and may be desirable since the rate of the hydrogenolysis reaction, which requires an ensemble of sites, is thereby diminished. It is also possible that the decrease in gas adsorption is due to the surface enrichment of Te or Sb on the Pt crystallites, since Te and Sb have lower surface free energies than platinum, if one estimates the surface free energy as one-quarter the component's heat of sublimation (*28, 29*). This enrichment hypothesis can be invoked only if the alloy crystallites formed are relatively large, because macroscopic thermodynamic properties may not apply to very small crystallites particularly under noninert gas environments (*29*). A further possibility could be electronic modification of the Pt on bonding with the second metal. This is possibly the main factor in the suppression of H_2 adsorption on vapor-deposited $PtTe/Al_2O_3$ catalysts. However, experiments using the isotopic dilution method indicated no electronic interactions between Pt and Sb.

It is evident that $PtTe/Al_2O_3$ catalysts prepared by the vapor deposition method differ from catalysts prepared by the coimpregnation method, as demonstrated by differences in their stabilities and capacities for H_2 adsorption. The instability of vapor-deposited catalysts prevented us from performing spectroscopic studies and also from obtaining absolute isomerization and cracking activities to correlate with Te content. Nevertheless, the modified catalysts displayed higher selectivities for isomerization than Pt/Al_2O_3.

The results obtained for the vapor-deposited $PtTe/Al_2O_3$ catalysts suggest that the unusual behavior of the catalysts is possibly due to the incorporation of carbonaceous deposits in the PtTe system since the most selective catalysts were formed only when *n*-hexane was added to the carrier gas used for tellurium deposition. There is no direct evidence of carbon participation in the formation of an active species, but consider the incorporation of Te into the Pt crystallites of the highly dispersed monometallic Pt/Al_2O_3 catalyst. As the vaporization of Te begins, less then 1% of the catalyst surface is occupied by the Pt metal. A legitimate question arises as to whether the vaporized Te molecules can "see" and alloy with the Pt clusters on the alumina surface. Weak physical adsorption of Te could explain the instability of Te in these catalysts. Possibly, the catalyst just consists of individual islands of Pt and Te clusters which are indifferent to the presence of H_2 or He. However, changes occur on the surface of the catalyst when it is in contact with a stream containing *n*-hexane. Carbonaceous deposits, by-products of hydrogenolysis reactions, may act as a linkage between Te and Pt, or may block the passage of Te in and out of the pores. Therefore, the catalyst system might be some form of Pt–Te–C, although the role of carbon in this catalyst and the details of alloy formation are highly speculative.

The influence of C deposits on the operation of reforming catalysts has been noted by several researchers. Lang *et al.* (*30*) showed that the rate of dehydrocyclization of *n*-heptanes and the selectivities for isomerization and hydrogenolysis in the reactions of *n*-heptanes are dependent upon the ordering of the carbonaceous layer. In an investigation of ethylene hydrogenation on a Pt(111) surface, Weinberg *et al.* (*31*) concluded that the carbonaceous layer is the catalytic site. Similar conclusions were also reached by Gardner and Hansen (*32*) using a tungsten-stepped surface. Völter *et al.* (*11*), in studying $PtSn/Al_2O_3$ and $PtPb/Al_2O_3$ catalysts, also pointed out that both C deposits and the second metal are responsible for the modified selectivities and activities of Pt sites.

Although coimpregnated $PtTe/Al_2O_3$ shows similar selectivity behavior to vapor-deposited $PtTe/Al_2O_3$, the formation of a stable PtTe cluster in the coimpregnated material which is somehow different from that of vapor-deposited $PtTe/Al_2O_3$ is indicated by the differences in their stabilities and capacities for H_2 adsorption. In addition, relatively stable alloys of Pt and Te on coimpregnated $PtTe/Al_2O_3$ must have been formed before the reaction experiments. Otherwise, a film of Te would have been visually observed on the downstream cold wall of the glass reactor during the activation periods and reaction experiments. Note that our experiments showed that Te is not strongly adsorbed on Al_2O_3 at 673 K.

The kinetic results for the coimpregnated catalysts can be explained as follows. The increase in selectivity for isomerization and concurrent decrease in hydrocracking selectivity can result from either an increase in isomerization activity or a decrease in hydrocracking activity. $PtTe/Al_2O_3$ with low Te content falls into the former category; the isomerization activity increases while the cracking activity is about the same as Pt/Al_2O_3. The increase in isomerization activity is possibly caused by electron donation from Te as determined by the ^{12}CO stretching frequency. High-content Te catalysts and all $PtSb/Al_2O_3$ fall into the latter category, for which geometric effects appear to predominate. Alloying of Pt with Te or Sb dilutes the active Pt surface such that ensemble size is reduced. Hydrocracking reactions typically take place on larger Pt ensembles than does isomerization; hydrocracking rates are therefore decreased. Barbier and Marecot (*33*) also attributed to the dilution effect the observed decrease in the rates of coking and hydrogenolysis reactions when Pt/Al_2O_3, Ir/Al_2O_3, or $PtIr/Al_2O_3$ catalysts were partially poisoned by sulfur, although they did not exclude other possibilities. Dehydrogenation reactions are typically similar to isomerization reactions with respect to their sensitivity to electronic effects and insensitivity to geometric effects. This assertion is borne out by the results of Table 5.

Electronic effects were not observed on any $PtSb/Al_2O_3$ catalyst, although it should be noted that the Sb/Pt ratios in all cases exceeded ≈ 0.10. The modifications in selectivity and activity for $PtSb/Al_2O_3$ resemble those of $PtTe/Al_2O_3$ with high Te content. Similar arguments presented previously for the behavior of high-Te-content $PtTe/Al_2O_3$ therefore apply to $PtSb/Al_2O_3$ as well.

Another notable, though less significant, effect of alloying is the roughly constant yield to benzene, compared to Pt/Al_2O_3. Isomerization and aromatization reactions generally proceed through a common cyclic intermediate, adsorbed methylcyclopentane, when acidic supports are used. This has also been shown to be true for certain alloy systems (*34*, *35*). A number of investigators (*7*, *9–12*) have found that alloying with Sb, Bi, Te, Sn, and Pb improves the yield to aromatics. The discrepancy between our results and their work may be an effect of the relatively nonacidic support used here, as it is generally believed that ring expansion from a five-member to a six-member ring requires the independent action of the metal and acidic centers of reforming catalysts (*36*, *37*). In fact, direct six-member ring closure, which occurs on the metal surface without involving acidic centers, is favored for metal catalysts on nonacidic supports (*38*, *39*). Because hydrogenolysis of MCP to form 2-MP and 3-MP can occur on metal (Pt) sites (*40*, *41*), it is not surprising that metal alloy catalysts on nonacidic supports display higher yields to isomerized rather than aromatized products. In addition, it appears that direct six-member ring closure is not affected by the addition of post-transition metal elements, as indicated by the roughly constant yield to benzene.

In summary, we conclude:

1. The addition of Te or Sb to Pt supported on relatively nonacidic alumina increases the isomerization selectivity and reduces the selectivity to hydrocracking products.

2. Alloy formation of vapor-deposited $PtTe/Al_2O_3$ may require carbonaceous deposits. The resulting alloy system behaves differently from coimpregnated $PtTe/Al_2O_3$.

3. For coimpregnated catalysts, electronic effects are recognizable in samples of low Te content and geometric effects are recognizable in all others. An electronic effect caused by Te to Pt electron donation increases the specific activities of isomerization and dehydrogenation reactions for catalysts of low Te/Pt ratio (0.06). A geometric effect, which may arise from partial poisoning of the Pt surface by added Te or Sb, decreases the specific activity of the hydrocracking reaction and is the dominant effect when the post-transition metal/Pt ratio exceeds ≈ 0.1. Although their mode of action differs, both effects result in improved selectivity to desired products. The kinetic data are in agreement with results using FTIR and the isotopic dilution method.

4. Isomerization reactions proceed through a five-member ring compound, adsorbed methylcyclopentane. The ring expansion of the five-member to a six-member ring apparently does not occur in this work because of the relatively low acidity of our supports. Direct six-member ring closure was responsible for the formation of the observed benzene and this mechanism was not affected by the addition of post-transition elements.

ACKNOWLEDGMENTS

The authors express appreciation to the Exxon Foundation for financial support. The assistance of Drs. Kenneth Riley and Al Schweizer at Exxon Research and Development in Baton Rouge Louisiana is especially appreciated.

REFERENCES

1. Biloen, P., Helle, J. N., Verbeek, H., Dautzenberg, F. M., and Sachtler, W. M. H., *J. Catal.* **63,** 112 (1980).
2. Carter, J. L., McVicker, G. B., Weissman, W., Kmak, W. S., and Sinfelt, J. H., *Appl. Catal.* **3,** 327 (1982).
3. Biloen, P., Dautzenberg, F. M., and Sachtler, W. M. H., *J. Catal.* **50,** 77 (1977).
4. Dejongste, H. C., Kuijers, K. J., and Ponec, V., *in* "Proceedings, 6th International Congress on Catalysis, London, 1976" (G. C. Bond, P. B. Wells, and F. C. Tompkins, Eds.), p. 915. The Chemical Society, London, 1976.
5. Ponec, V., and Sachtler, W. M. H., *J. Catal.* **24,** 250 (1972).
6. Soma-Noto, Y., and Sachtler, W. M. H., *J. Catal.* **32,** 315 (1974).
7. Thoang, H. S., Lanh, H. D., and Völter, S., *in* "Proceedings, 8th International Congress on Catalysis, Berlin, 1984," p. 2–509. Dechema, Frankfurt-am-Main, 1984.
8. Coughlin, R. W., Hasan, A., and Kawakami, K., *J. Catal.* **88,** 163 (1984).
9. Eberly, P. E., Jr., U.S. Patent 4,169,785 (1979).
10. Brignac, D. G., and Swan, G. A., U.S. Patent 4,485,188 (1984).
11. Völter, J., Lietz, G., Uhlemann, M., and Hermann, M., *J. Catal.* **68,** 42 (1981).
12. Davis, B.H., Westfall, G.A., Watkins, J., and Pezzanite, J., *J. Catal.* **42,** 247 (1976).
13. Goldwasser, J., Arenas, B., Bolivar, C., Castro, G., Bodriguez, A., Fleitas, A., and Giron, J., *J. Catal.* **100,** 75 (1986).
14. Benesi, H. A., Curtis, R. M., and Studer, H. P., *J. Catal.* **10,** 328 (1968).
15. Dorling, T. A., Lynch, B. W. J., and Moss, R. L., *J. Catal.* **20,** 190 (1971).
16. Adkins, S. R., and Davis, B. H., *J. Catal.* **89,** 371 (1984).
17. Dorling, T. A., Burlace, C. J., and Moss, R. L., *J. Catal.* **12,** 207 (1968).
18. Freel, J., *J. Catal.* **25,** 149 (1972).
19. Spenadel, L., and Boudart, M., *J. Phys. Chem.* **64,** 204 (1960).
20. Sinfelt, J. H., Carter, J. L., and Yates, D. J. C., *J. Catal.* **24,** 283 (1972).
21. Wheeler, A., *in* "Catalysis" (P. H. Emmett, Ed.), Vol. 2. Reinhold, New York, 1955.
22. Bastein, A. G. T. M., Toolenaar, F. J. C. M., and Ponec, V., *J. Catal.* **90,** 88 (1984).
23. Toolenaar, F. J. C. M., Stoop, F., and Ponec, V., *J. Catal.* **82,** 1 (1983).
24. Stoop, F., Toolenaar, F. J. C. M., and Ponec, V., *J. Catal.* **73,** 50 (1982).
25. Hammaker, R. M., Francis, S. A., and Eischens, R. P., *Spectrochim. Acta* **21,** 1295 (1965).
26. Palazov, A., Bonev, Ch., Kadinov, G., Shopov, D., Lietz, G., and Völter, J., *J. Catal.* **71,** 1 (1981).
27. Apesteguia, C. R., Brema, C. E., Garetto, T. F., Borgna, A., and Parera, J. M., *J. Catal.* **89,** 52 (1984).
28. Somorjai, G. A., *in* "Principles of Surface Chem-

istry," pp. 56–64. Prentice–Hall, Englewood Cliffs, NJ, 1972.

29. Williams, F. L., and Danson, D., *Surf. Sci.* **45,** 377 (1974).
30. Joyner, R. W., Lang, B., and Somorjai, G. A., *J. Catal.* **27,** 405 (1972).
31. Weinberg, W. H., Deans, H. A., and Merrill, R. P., *Surf. Sci.* **41,** 312 (1974).
32. Gardner, N. C., and Hansen, R. S., *J. Phys. Chem.* **74,** 3298 (1970).
33. Barbier, J., and Marecot, P., *J. Catal.* **102,** 21 (1986).
34. Coq, B., and Figueras, F., *J. Catal.* **85,** 197 (1984).
35. O'Cinneide, A., and Gault, F. G., *J. Catal.* **37,** 311 (1975).
36. Sinfelt, J. H., *Adv. Chem. Eng.* **5,** 37 (1964).
37. Parera, J. M., Beltramini, J. N., Querini, C. A., Martinelli, E. E., Churin, E. J., Aloe, P. E., and Figoli, N. S., *J. Catal.* **99,** 39 (1986).
38. Davis, B. H., *J. Catal.* **42,** 376 (1976).
39. Dautzenberg, F. M., and Platteeuw, J. C., *J. Catal.* **19,** 41 (1970).
40. Barron, Y., Maire, G., Muller, J. M., and Gault, F. G., *J. Catal.* **5,** 428 (1966).
41. Corolleur, C., Corrolleur, S., and Gault, F. G., *J. Catal.* **24,** 385 (1972).